ARTICLE NO. 79-0680R

J80-092

Applications of Velocity Potential Function to Acoustic Duct Propagation Using Finite Elements

20001

K. J. Baumeister*
NASA Lewis Research Center, Cleveland, Ohio
and
R. K. Majjigi†
General Electric Co., Cincinnati, Ohio

A finite element velocity potential program has been developed for NASA Lewis at the Georgia Institute of Technology to study acoustic wave propagation in complex geometries. For irrotational flows, relatively low sound frequencies, and plane wave input, the finite element solutions show significant effects of inlet curvature and flow gradients on the attenuation of a given acoustic liner in a realistic variable area turbofan inlet. In addition, as shown in the paper, the velocity potential approach can not be used to estimate the effects of rotational flow on acoustic propagation since the potential acoustic disturbances propagate at the speed of the media in sheared flow. Approaches are discussed that are being considered for extending the finite element solution to include the far field as well as the internal portion of the duct. A new matrix partitioning approach is presented that can be incorporated in previously developed programs to allow the finite element calculation to be marched into the far field. The partitioning approach provides a large reduction in computer storage and running times.

Nomenclature

C_1 = constant of integration, N/m^2, Eq. (22)
C_2, C_3 = constants of integration, m/s, Eqs. (23) and (24)
c_0 = velocity of sound, m/s
D_0 = diameter at rotor position, m
f = frequency, Hz
H = height of duct, m
i = $\sqrt{-i}$
K = number of grid points in axial direction
L = length of duct, m
M = Mach number of axial mean flow, U/c_0
m = spinning mode number
p = acoustic pressure, $p(x,y,t)$; N/m^2
p_0 = entrance acoustic pressure, $p_0(0,y,t)$; N/m^2
p^0 = spatial acoustic pressure, $p^0(x,y)$; N/m^2
r = radial coordinate, m
t = time, s
U = axial mean flow velocity, $U(x,y)$; m/s
u = acoustic axial velocity, $u(x,y,t)$, m/s
u^0 = spatial acoustic axial velocity, $u^0(x,y)$; m/s
V = transverse mean flow velcoity, $V(x,y)$; m/s
v = acoustic transverse velocity, $v(x,y,t)$; m/s
v^0 = spatial acoustic transverse velocity, $v^0(x,y)$; m/s
x = axial coordinate, m
y = transverse coordinate, m
Z = impedance, g/cm^2 s
Z_{eff} = effective impedance, g/cm^{2}s
z = axial position
ζ = specific acoustic impedance
η = dimensionless frequency $D_0 f/c_0$ or Hf/c_0
θ = angular position, rad
ρ_0 = density, g/m^3
Φ = steady potential function, $\Phi(x,y)$; m^2/s
Φ^* = potential function, $\Phi^*(x,y,t)$; m^2/s
φ = acoustic potential function, $\varphi(x,y,t)$; m^2/s
φ^0 = spatial acoustic potential function, $\varphi^0(x,y)$; m^2/s
ω = angular frequency, rad/s

Subscripts

$\left\{ \right\}_{x \atop xx}$ = derivatives with respect to x (similar for y and t)

Introduction

WHEN using numerical techniques in calculating acoustic waves propagating in ducts (such as finite elements in Refs. 1-3 and finite differences in Refs. 4-6) the velocity potential formulation of the acoustic wave equation[1] offers many advantages over the conventional linearized gas equation.[2] For two-dimensional flows, the velocity potential approach reduces the computer storage and running time by an order of magnitude compared to the more general linearized gas equation approach. Since the flow into an inlet is usually modeled by potential flow (excluding the boundary layer), the acoustic velocity potential is ideally suited for acoustic inlet calculations.

On the other hand, when rotational flow exists in the inlet (wall and centerbody boundary layers), the accuracy of a potential flow calculation is questionable. The first purpose of this paper was to investigate the limitations of shear on the potential flow formulation and to suggest a means of extending the potential flow finite element analysis to incorporate sheared flow. A second purpose of this paper was to determine the sensitivity of an acoustic liner to variations in area and flow experienced in a typical engine inlet.[7] This was accomplished using the finite element velocity potential computer program developed by the Georgia Institute of Technology for NASA Lewis Research Center written under NASA Lewis grant (NAS-3036).

Finally, finite elements can include simultaneously both the far field and internal ducting of a turbofan engine. For example, in the absence of flow, a formulation of a finite

Presented as Paper 79-0680 at the AIAA 5th Aeroacoustics Conference, Seattle, Wash., March 12-14, 1979; submitted April 11, 1979; revision received Sept. 13, 1979.

Index category: Aeroacoustics.

*Aerospace Engineer.
†Engineer. Member AIAA.

element approach for sound propagation in the near field of an infinite baffle with an embedded circular piston was presented in Ref. 8. Although the finite element approach is relatively easy to formulate, core storage requirements and long run times presently prevent the application of the finite element approach to simultaneously including both the inlet and far field in a single calculation. In Ref. 1, for example, by structuring the column matrix of modal unknowns to successively be the real and then the imaginary part of the acoustic potential at a node, the global matrix is well banded. Even so, the formulation of Ref. 1 was limited to 270 elements. Reference 3 improved the matrix structure by using a complex solution technique which reduced the bandwidth of the matrix even further; however, 150 total elements were the maximum quoted in the paper.

The third purpose of this paper, therefore, is to discuss current work for extending finite element velocity potentials from the internal portion of the duct into the far field. In particular, a new numerical partitioning method is presented which is suited for extending the solution from the internal portion of the duct into the far field.

Sheared Mean Flow

Rotational velocity fields exist for sheared viscous flows in the inlet along the walls of a turbofan cowl and along its centerbody. The complete acoustic equations for sheared viscous flows were developed by Munger and Gladwell.[9] By common practice, the viscous terms in the linearized acoustic equations are neglected and the inviscid acoustic equations are solved using the mean flow velocities that result from a consideration of viscosity only on the mean flowfield. Similarly, because of the significant computational advantage of the acoustic potential formulation, it would be desirable if the existing potential wave program could be extended to include boundary layer flows. First, the fully irrotational acoustic flow equations will be presented. Next, this paper will develop the acoustic flow equations for a rotational mean flow field with an irrotational acoustic field. The consequence of such an assumption is discussed and conclusions are made about the use of the acoustic potential function to model sheared flows.

Irrotational Mean and Irrotational Acoustic Flowfields

For two-dimensional flows, the velocity potential representation of the inviscid momentum and mass continuity equations can be written as (Ref. 10, p. 76)

$$\Phi^*_{tt}+2\Phi^*_x\Phi^*_{xt}+2\Phi^*_y\Phi^*_{ty}+\Phi^{*2}_x\Phi^*_{xx}+2\Phi^*_x\Phi^*_y\Phi^*_{xy}+\Phi^{*2}_y\Phi^*_{yy}=c_0^2\Phi^*_{xx}+c_0^2\Phi^*_{yy} \tag{1}$$

where Φ^* is the velocity potential. The symbols are defined in the Nomenclature. To keep the analysis simple, the rectangular coordinate system is used rather than a more general coordinate system. The velocity potential Φ^* is assumed to be composed of a steady potential Φ and an acoustic potential φ:

$$\Phi^*(x,y,t)=\Phi(x,y)+\varphi(x,y,t) \tag{2}$$

The mean flow velocities are of the form

$$U=\Phi_x=U(x,y) \tag{3}$$

$$V=\Phi_y=V(x,y) \tag{4}$$

and a constant speed of sound c_0 is assumed. With these assumptions, and by dropping those terms which, according to the assumption of small perturbation, may be regarded as negligible compared to the remaining terms, Eq. (1) reduces to

$$(1-M^2)\varphi_{xx}+\varphi_{yy}-2\frac{M}{c_0}\varphi_{xt}-2M\frac{\partial M}{\partial y}\varphi_y-\frac{1}{c_0^2}\varphi_{tt}=\frac{V^2}{c_0^2}\varphi_{yy}+\frac{2V}{c_0^2}\varphi_{yt}+\frac{2V}{c_0}\frac{\partial M}{\partial y}\varphi_x+2M\frac{V}{c_0}\varphi_{xy}+2\frac{V}{c_0^2}\frac{\partial V}{\partial y}\varphi_y \tag{5}$$

where the mean flow velocities are related by the irrotationality condition

$$c_0\frac{\partial M}{\partial y}=\frac{\partial V}{\partial x} \tag{6}$$

Parallel shear flow with $M(y)$ and $V=0$ is used to approximate boundary layer flows. In this case, Eq. (5) reduces to

$$(1-M^2)\varphi_{xx}+\varphi_{yy}-2\frac{M}{c_0}\varphi_{xt}-2M\frac{\partial M}{\partial y}\varphi_y-\frac{1}{c_0^2}\varphi_{tt}=0 \tag{7}$$

However, Eq. (7) violates the irrotationality assumption which was used to establish Eq. (1) since Eq. (6) is no longer satisfied. Could, however, Eq. (7) be used to approximate a shear flowfield? Equation (7) is similar to the Pridmore-Brown[11] shear flow equation, except the Pridmore-Brown equation has two dependent variables. When the wave equation is expressed in one dependent variable, it becomes third order (Ref. 12, Eq. 1.22, p. 9). Therefore, Eq. (7) may alter the true physics of the acoustic propagation. It would be difficult to evaluate the effect of this approximation from numerical solutions. Consequently, a derivation will now be made assuming an acoustic potential in a parallel sheared mean flow to determine whether or not valid results are obtained from a solution to Eq. (7).

Rotational Mean Flow and Irrotational Acoustic Propagation

Because of the significant computational advantages of the acoustic potential formulation, an attempt will be made to extend the existing potential wave program to include the case of boundary layer flows that exist along the engine walls and centerbodies. To do this in a rigorous manner, one starts with the linearized gas dynamic equations for a rotational flowfield.

For the simple case of a rectangular coordinate system and isentropic ($p=c_0^2\rho$) parallel sheared mean flow [$U=U(y)$; $V=0$], the governing gas dynamic equations[13] become

Continuity

$$\frac{\partial p}{\partial t}+U\frac{\partial p}{\partial x}+\rho_0 c_0^2\left(\frac{\partial u}{\partial x}+\frac{\partial v}{\partial y}\right)=0 \tag{8}$$

x momentum

$$\frac{\partial u}{\partial t}+U\frac{\partial u}{\partial x}+v\frac{\partial U}{\partial y}=-\frac{1}{\rho_0}\frac{\partial p}{\partial x} \tag{9}$$

y momentum

$$\frac{\partial v}{\partial t}+U\frac{\partial v}{\partial x}=-\frac{1}{\rho_0}\frac{\partial p}{\partial y} \tag{10}$$

A solution to Eqs. (8-10) will, of course, require greater computer storage and operating time than Eq. (7) since the number of dependent variables has increased from one (φ) to three (p,u,v). Now, the mean flow is considered to be rotational and the acoustic field is assumed to be irrotational such that

$$u=\frac{\partial\varphi}{\partial x} \tag{11}$$

$$v = \frac{\partial \varphi}{\partial y} \tag{12}$$

This assumption reduces Eqs. (8-10) to

$$\frac{\partial p}{\partial t} + U\frac{\partial p}{\partial x} + c_0^2 \rho_0 (\varphi_{xx} + \varphi_{yy}) = 0 \tag{13}$$

$$\varphi_{tx} + U\varphi_{xx} + \varphi_y \frac{\partial U}{\partial y} = -\frac{1}{\rho_0}\frac{\partial p}{\partial x} \tag{14}$$

$$\varphi_{ty} + U\varphi_{xy} = -\frac{1}{\rho_0}\frac{\partial p}{\partial y} \tag{15}$$

Equations (13-15) can not be combined to obtain a second-order differential wave equation in the dependent variable. However, differentiating Eq. (14) with respect to y and Eq. (15) with respect to x and subtracting one equation from the other yields

$$(\varphi_{xx} + \varphi_{yy})\frac{\partial U}{\partial y} + \varphi_y \frac{\partial^2 U}{\partial y^2} = 0 \tag{16}$$

which is the governing equation for describing an irrotational acoustic disturbance in a parallel mean shear flow. Since Eq. (16) contains no derivatives with respect to time, the irrotationality assumption changes the nature of the propagation equation.

The significance of Eq. (16) can be understood clearly by considering the simple case of a linear shear profile ($\partial^2 U/\partial y^2 = 0$). In this simpler but practical case, Eq. (16) reduces to

$$\varphi_{xx} + \varphi_{yy} = 0 \tag{17}$$

or if a harmonic time dependence is assumed

$$\varphi = \varphi^0 e^{-i\omega t} \tag{18}$$

then

$$\varphi^0_{xx} + \varphi^0_{yy} = 0 \tag{19}$$

Thus, the governing equation for the velocity potential becomes Laplace's equation, which indicates a diffusive propagation rather than a wave-like propagation. The effect of this propagation on p and the acoustic velocities will now be considered.

The continuity equation, Eq. (13), simplifies by the use of Eq. (17) to

$$\frac{\partial p}{\partial t} + U\frac{\partial p}{\partial x} = 0 \tag{20}$$

Again, assuming that $p = p^0 e^{-i\omega t}$, Eq. (20) yields

$$p^0 + i\frac{U}{\omega}\frac{\partial p^0}{\partial x} = 0 \tag{21}$$

For a plane pressure wave at $x = 0$, a solution for p^0 from Eq. (21) is simply

$$p^0 = C_1 e^{i\omega x/U} \tag{22}$$

Similarly assuming $u = u^0 e^{-i\omega t}$ and $v = v^0 e^{-i\omega t}$ and substituting Eq. (22) into Eqs. (14) and (15) yields after integration

$$u^0 = e^{i\omega x/U}\left[C_3 - \frac{C_1 i\omega x}{\rho_0 U^2} - \frac{1}{U}\frac{\partial U}{\partial y}\left(C_2 x + \frac{iC_1\omega x^3}{6\rho_0 U^3}\frac{\partial U}{\partial y}\right)\right] \tag{23}$$

$$v^0 = e^{i\omega x/U}\left(C_2 + \frac{iC_1\omega}{2\rho_0 U^3}\frac{\partial U}{\partial y}x^2\right) \tag{24}$$

These solutions of the continuity and momentum equations have lead to the fact that

$$p, u, v, \alpha e^{(i\omega/U)x} \tag{25}$$

that is, only forward propagating perturbation pressure p and velocities will exist and they will propagate at the speed of the medium flow U. Therefore, Eq. (16) does not have an acoustic solution; consequently, the potential flow solution cannot be used to estimate the effects of shear even in an approximate manner.

For the case of boundary layer flow, however, a procedure based on the Goldstein-Rice analysis[14] might be used for predicting the attenuation with shear flow in conjunction with the potential finite element method for turbofan inlets. In Ref. 14, an exact analytical solution to the equations governing the propagation of sound in a uniform shear layer is used to develop a closed form solution for acoustic wall impedance which accounts for both the duct liner and the presence of a boundary layer in the duct. Therefore, in a turbofan inlet, the impedance at the wall can be transformed into an effective impedance, Z_{eff}, at the edge of the boundary layer using the results of Ref. 14. This effective impedance could be used as the boundary condition for the potential flow calculation. The procedure is approximate because the calculation assumes a uniform boundary layer in the axial direction. For a growing boundary layer, the transform could be assumed to apply locally. In any event, this procedure represents a simple effective way of accounting for shear with a potential flow program.

Attenuation Sensitivity to Variable Area

The theory used for the design of acoustic liners for turbofan inlets without splitter rings has used a cylindrical duct for a model. As mentioned earlier, the present paper will estimate the sensitivity of duct attenuation to inlet curvature, centerbody and flow gradients (irrotational) for a typical turbofan inlet. To accomplish this task, a number of acoustic calculations are performed on the soft-walled turbofan inlet shown in Fig. 1. This inlet geometry is similar to the quiet, clean, short-haul experimental engine (QCSEE) inlet which was designed to suppress inlet-emitted engine machinery noise using a high throat Mach number and thus has somewhat more curvature than a conventional inlet. In this case, the velocity potential finite element program of Ref. 1 was modified to include quadratic elements.

The governing equations in the program are developed from the axisymmetric cylindrical coordinate form of Eqs. (1-6). The exact form of φ is

$$\varphi(r,\theta,z,t) = \varphi^0(r,z)e^{-i(\omega t - m\theta)} \tag{26}$$

The detailed governing equations will not be presented here since they are fully documented in Ref. 1. Boundary layers are not considered in the calculation because, as was just shown, the program is limited to only irrotational flowfields.

At the present time, the frequency range and radial mode content is limited by the maximum number of elements which the computer can handle. The analysis considers plane wave input with dimensionless frequencies of η up to 2. In this case, seven elements were used to resolve the radial modes and fourteen elements were used to resolve axial variations. The acoustic design of an actual inlet will, of course, consider much higher frequencies. Unfortunately, at the present time finite element schemes can not handle high frequencies. Therefore, this analysis only investigates low frequency noise in variable area inlets. This might be corrected by adapting the wave envelope technique of Ref. 6 to this problem. The wave envelope technique can handle high frequencies with much

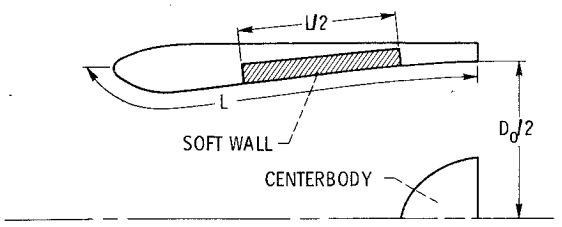

Fig. 1 Variable area inlet.

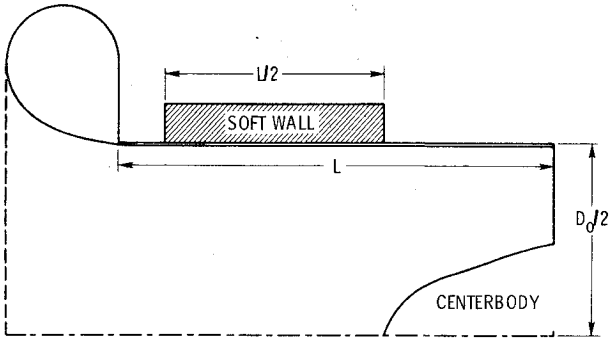

Fig. 2 Bellmouth inlet.

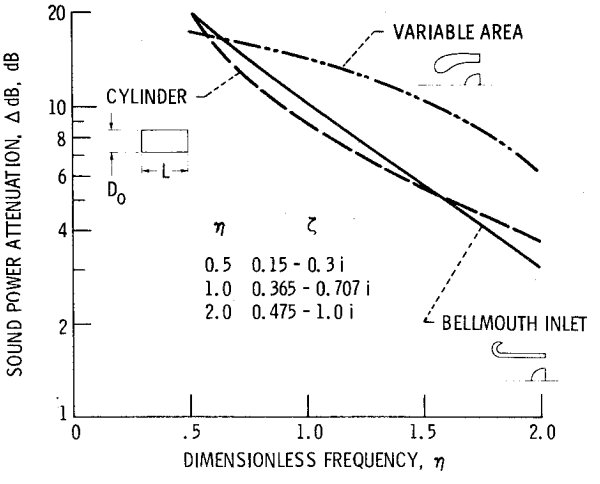

Fig. 3 Sound attenuation for inlets with a treatment L/D_0 of 0.5 for a plane acoustic velocity source with zero mean flow.

fewer elements.

Attenuation calculations for a variable area inlet, a straight open cylinder, and a bellmouth (Fig. 2) all with an L/D of 1 are presented in Fig. 3. The ratio of treatment length to duct diameter in these cases is 0.5. The soft wall extends over half the length of the duct beginning at the nose of the centerbody. With this geometry, the infinite uniform cylindrical duct model could be expected to give a reasonable estimate of the attenuation. The results displayed in Fig. 3 are for no mean flow. The effects of flow will be considered later. The impedance values chosen are the same for each inlet at a particular frequency. They are listed in Fig. 3. The impedance values chosen in the calculation approximate the optimum impedance (maximum attenuation) for a plane pressure wave input into a long circular duct. A plane acoustic velocity is used as the source with a $\rho_0 c_0$ exit impedance.

The effect of inlet curvature and the centerbody on the duct attenuation can be ascertained by comparison of the various curves in Fig. 3 representing each inlet. The cylinder and bellmouth inlets give approximately the same attenuation as a function of frequency. Since the bellmouth is of uniform circular geometry, the effect of the short centerbody on the

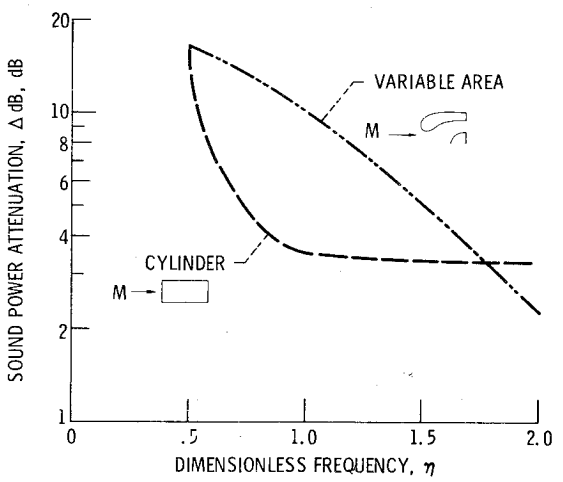

Fig. 4 Sound attenuation for inlets with a treatment L/D_0 of 0.5 for a plane acoustic pressure source with a fan face Mach number of 0.52.

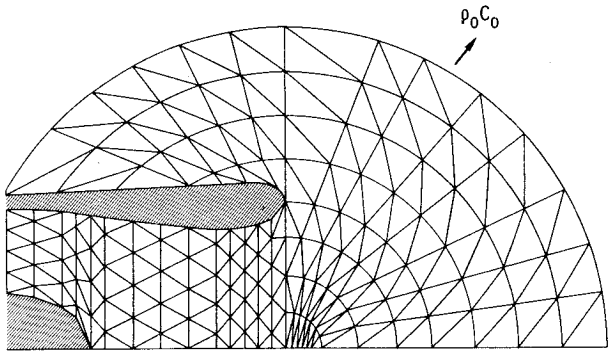

Fig. 5 Extending finite elements into far field.

results appears to be insignificant in this no-flow situation. The large area variation of the other inlet, however, does significantly affect the results. This suggests that reflections in this inlet may be important.

Figure 4 compares preliminary attenuation calculations for the variable area inlet and a cylinder inlet in a flow situation. The fan plane Mach number for the variable area inlet was 0.52 with an average Mach number of 0.579 at the soft wall section of the inlet, as calculated by one-dimensional isentropic gas dynamic relations. The Mach number in the cylinder was also chosen to be 0.579. The impedance values used in these calculations were those listed in Fig. 3 divided by $(1-M)^2$ with M equal to 0.579. Again, as seen in Fig. 4, the QCSEE inlet differs considerably from the cylinder results.

In Fig. 4, the flattening of the cylinder attenuation curve probably results because the impedance values chosen are not at the optimum for this Mach number. However, the important point is that for the same value of impedance, area variations can significantly change the calculated attenuation.

Far-Field Radiation

As mentioned in the Introduction, this section will be concerned with current ideas for extending finite elements from the internal portion of the duct into the far field. Under a three-year extension of NASA Lewis grant NAS-3036, which will run from Nov. 1978 to Oct. 1981, Zinn and Sigman will be developing methods for extending their finite element analysis into the far field. First, a small effort will be devoted to more accurately and efficiently specifying the steady flowfield around an inlet in a form compatible with the acoustic calculations. However, the majority of the work effort in this grant will be devoted toward the calculation of acoustic properties of the inlet and the associated external region.

The direct extension of finite elements into the far field is illustrated in Fig. 5. The number of elements greatly increases the further the analysis is carried from the inlet. Therefore, this approach requires very efficient ways of storing and solving the finite element global matrix. Considerable effort should be devoted to the direct method, since improved handling of the elements will benefit far-field approaches as well as improve capabilities for present induct analysis. As mentioned earlier, to handle higher frequencies inside the duct, greater efficiency is still needed to increase the number of internal elements.

A new numerical partitioned matrix approach is now presented which allows far field acoustic problems to be subdivided into smaller independent and thus more manageable problems. This procedure can be incorporated in previously developed programs with minimal effort. Sample calculations for a two-dimensional rectangular coordinate soft wall duct with uniform flow are presented later to illustrate the method. Before discussing the partition approach, the boundary conditions used in a typical numerical acoustic analysis will be reviewed briefly.

Finite element or finite difference analyses usually require an acoustic pressure or velocity distribution as the entrance boundary condition and some assumed impedance as the exit boundary condition. For plane wave propagation without mean flow in a finite straight duct, the acoustic impedance at the outlet of the duct is nearly $\rho_0 c_0$ for dimensionless frequencies η greater than 1.5, as shown in Refs. 15 and 16. Figures 6a depicts the geometry and appropriate boundary conditions for a rectangular duct with these conditions. For spinning or higher order modes, the exit impedance values of Refs. 1 or 3 could be used.

The basic idea for the partitioning approach comes from the marching technique developed in Ref. 17. As shown in Ref. 17, in regions where reflections are small, the $\rho_0 c_0$ exit impedance was nearly constant along the entire length of the duct. Thus, the internal portion of the duct and the far field can be separated into regions and solved independently. The exit pressure calculated in the first region is used as the initial condition for the pressure in the second region, and so forth.

For high-frequency sound where reflections are small, the partition could be taken at the exit, as shown in Fig. 6a. For low frequency sound or for an arbitrary input with multiple nodes, the partition should be moved from the exit to the far field where the $\rho_0 c_0$ impedance is valid, as shown in Fig. 6b.

The number of partitions used in the far field could be as many as desired, as illustrated in Fig. 7. The total computer storage is reduced by approximately the square of the number of partitions. If seven partitions were used, this would be a storage reduction of about 50. Furthermore, since the solution times are roughly proportional to the total number of nodes cubed (Ref. 18, p. 261), the total running time should also be reduced by a factor of 50.

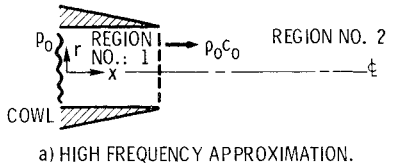

a) HIGH FREQUENCY APPROXIMATION.

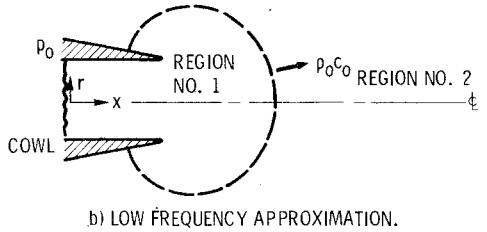

b) LOW FREQUENCY APPROXIMATION.

Fig. 6 Application of partitioning to engine inlets.

To illustrate the capabilities of the partitioning technique, the noise attenuation at the optimum impedance (point of maximum attenuation in the impedance plane) is calculated using finite difference theory for a two-dimensional rectangular duct with an L/H of 3.43, a uniform Mach number of 0.3 and a plane wave input.

Dimensionless frequencies of η equal to 1.5 and 2 are considered. As shown in Ref. 16, a dimensionless frequency of 1.5 is just sufficiently high so that a $\rho_0 c_0$ exit impedance is valid. In these two cases, as discussed in Ref. 17, the $\rho_0 c_0$ exit impedance is nearly constant along the entire duct. Therefore, the duct can be partitioned. Figure 8 shows the duct with seven assumed partitions represented by the dash vertical lines.

Figure 9 displays the calculated maximum sound power attenuations for η equal to 1.5 and 2. The number of axial grid points K have been varied to check for convergence. The results converge to the analytically predicted attenuation[19] which apply to ducts of infinite length. Without partitions, approximately 100 axial grid points are required, while with partitioning only 20 axial grid points are needed in each partitioned element. As mentioned in the body of the report, this reduces the storage requirement by a factor of 50 and the total running time also by a factor of 50. Of course, the method must be tested over a greater range of acoustic variables to check its validity.

Concluding Remarks

The finite element velocity potential program developed for NASA Lewis by Georgia Institute of Technology is suitable for handling low-frequency acoustic wave propagation in ducts with area variations, centerbodies, and axial variations in wall impedance whenever irrotational flow gradients exist in a duct. Consequently, the program is ideally suited for handling low-frequency acoustic wave propagation in a

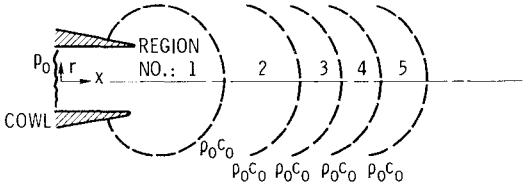

Fig. 7 Multi-partitions used in far-field analysis.

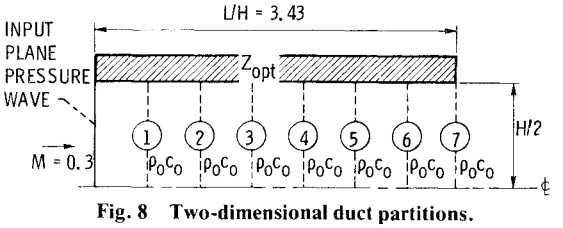

Fig. 8 Two-dimensional duct partitions.

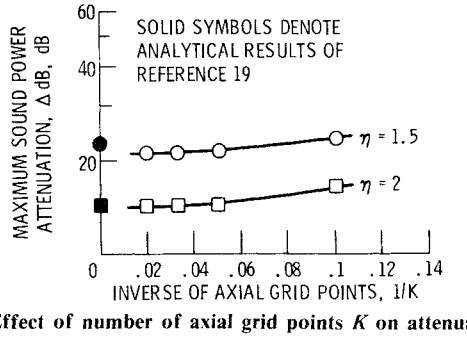

Fig. 9 Effect of number of axial grid points K on attenuation for seven partitions in a soft wall duct $L/H = 3.43$, $M = 0.3$ and wall impedance at optimum value for plane wave input.

turbofan inlet in which the mean flowfield is predominantly irrotational and two dimensional.

Unfortunately, as shown herein, the velocity potential program can not be used directly to estimate the effects of wall shear layers on acoustic propagation. However, a boundary layer correction based on the Goldstein-Rice analysis is suggested for predicting attenuation in soft wall ducts.

In some sample calculations for a variable area inlet, the combined effect of inlet curvature and flow gradients was shown to have significant effects on the attenuation of a given acoustic liner for very low frequencies. The short centerbody did not seem to have such effect.

Finally, approaches were discussed that are actively being considered for extending the finite element solution to include the far field as well as the internal portion of the duct. A new matrix partitioning approach was presented that can be incorporated in previously developed programs which may allow the finite element calcuation to be marched into the far field. The partitioning approach provides a large reduction in computer storage and running times.

References

[1] Sigman, R. K., Majjigi, R. K., and Zinn, B. T., "Use of Finite Element Techniques in the Determination of the Acoustic Properties of Turbofan Inlets," AIAA Paper 77-18, Jan. 1977.

[2] Abrahamson, A. L., "A Finite Element Algorithm for Sound Propagation in Axisymmetric Ducts Containing Compressible Mean Flow," AIAA Paper 77-1301, Oct. 1977.

[3] Tag, I. A. and Lumsdaine, E., "An Efficient Finite Element Technique for Sound Propagation in Axisymmetric Hard Wall Ducts Carrying High Subsonic Mach Number Flows," AIAA Paper 78-1154, July 1978.

[4] Baumeister, K. J. and Bittner, E. C., "Numerical Simulation of Noise Propagation in Jet Engine Ducts," NASA TN D-7339, 1973.

[5] Quinn, D. W., "A Finite Difference Method for Computing Sound Propagation in Non-Uniform Ducts," AIAA Paper 75-130, Jan. 1975.

[6] Baumeister, K. J., "Finite-Difference Theory for Sound Propagation in a Lined Duct with Uniform Flow Using the Wave Envelope Concept," NASA TP-1001, Aug. 1977.

[7] Miller, B. A., Dastoli, B. J., and Wesoky, H. L., "Effect of Entry-Lip Design on Aerodynamics and Acoustics of High-Throat-Mach Number Inlets for Quiet, Clean, Short-Haul Experimental Engine," NASA TM X-3222, May 1975.

[8] Kagawa, Y., Yamabuchi, T., and Mori, A., "Finite Element Simulation of an Axisymmetric Acoustic Transmission System with a Sound Absorbing Wall," *Journal of Sound and Vibration*, Vol. 53, Aug. 1977, pp. 357-374.

[9] Mungur, P. and Gladwell, G.M.L., "Acoustic Wave Propagation in a Sheared Fluid Contained in a Duct," *Journal of Sound and Vibration*, Vol. 9, Jan. 1969, pp. 28-48.

[10] Pai, S., *Introduction to the Theory of Compressible Flow*, D. Van Nostrand, Princeton, 1959.

[11] Pridmore-Brown, D. C., "Sound Propagation in a Fluid Flowing Through an Attenuating Duct," *Journal of Fluid Mechanics*, Vol. 4, Pt. 4, Aug. 1958, pp. 393-406.

[12] Goldstein, M. E., *Aeroacoustics*, McGraw-Hill, New York, 1976.

[13] Savkar, S. D., "Propagation of Sound in Ducts with Shear Flow," *Journal of Sound and Vibration*, Vol. 19, Dec. 1971, pp. 355-372.

[14] Goldstein, M. and Rice, E., "Effect of Shear on Duct Wall Impedance," *Journal of Sound and Vibration*, Vol. 30, Sept. 1973, pp. 79-84.

[15] Meyer, W. L., Bell, W. A., Zinn, B. T., and Stalybrass, M. P., "Boundary Integral Solutions of Three Dimensional Acoustic Radiation Problems," *Journal of Sound and Vibration*, Vol. 59, July 1978, pp. 245-262.

[16] Majjigi, R. K., "Application of Finite Element Techniques in Predicting the Acoustic Properties of Turbofan Inlets," Ph.D. Thesis, Georgia Institute of Technology, submitted for approval 1979.

[17] Baumeister, K. J., "Numerical Spatial Marching Techniques in Duct Acoustics," *Journal of Acoustical Society of America*, Vol. 65, Feb. 1979, pp. 297-306.

[18] McCracken, D. D. and Dorn, W. S., *Numerical Methods and Fortran Programing, With Applications in Engineering and Science*, Wiley, New York, 1964.

[19] Motsinger, R. E., Kraft, R. E., Zwick, J. W., Vukelich, S. I., Minner, G. L., and Baumeister, K. J., "Optimization of Suppression for Two-Element Treatment Liners for Turbomachinery Exhaust Ducts," General Electric Co., Cincinnati, Ohio, R76AEG256, April 1976; also NASA-CR-134997.